

Supporting Information

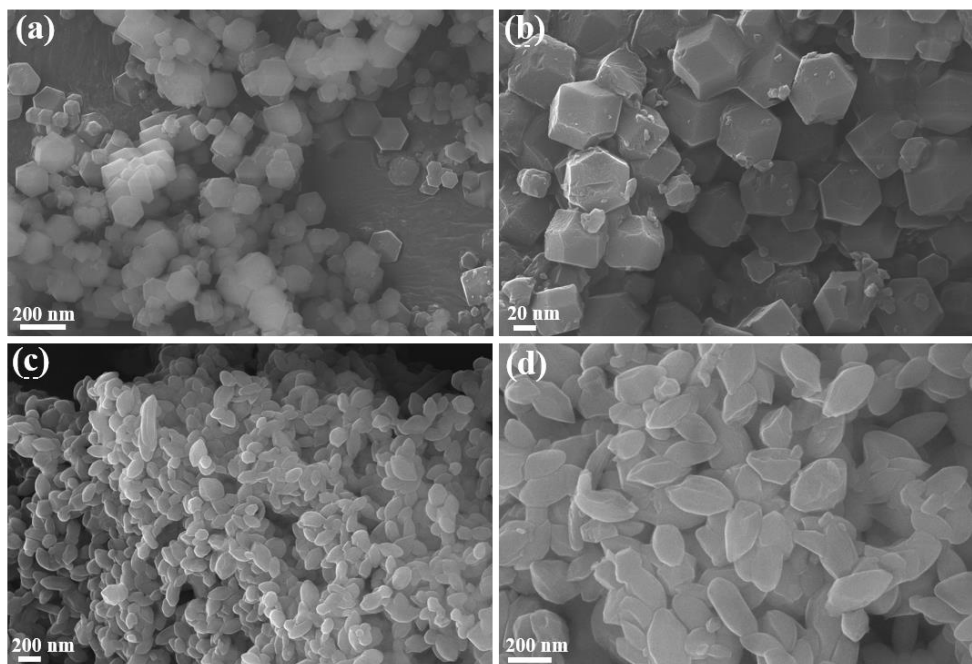


Figure S1: SEM images of ZIF-8 (a, b) and Fe/Mn-MOF (c, d).

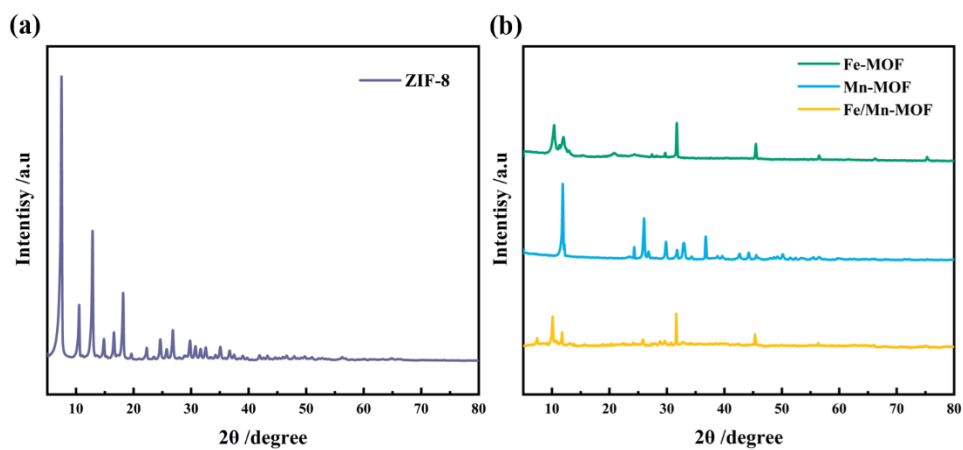


Figure S2: XRD patterns of ZIF-8 (a) and Fe-MOF, Mn-MOF and Fe/Mn-MOF (b).

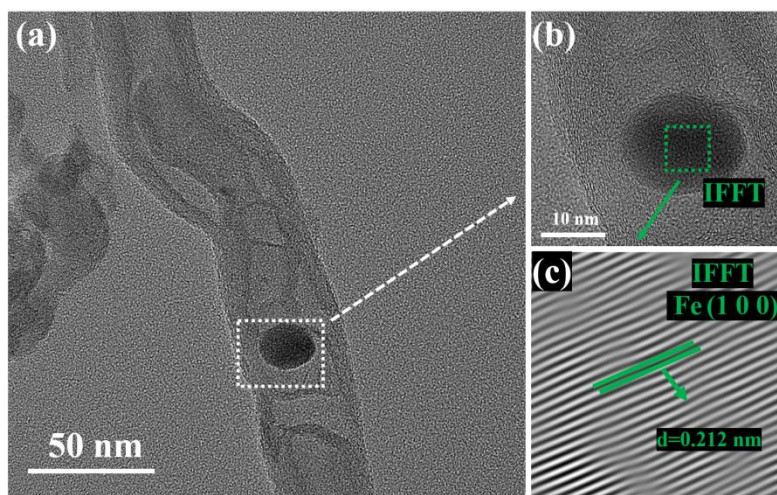


Figure S3: TEM image (a), HRTEM image (b) and IFFT image of marked region of (b) for Z-Fe1Mn1-NC.

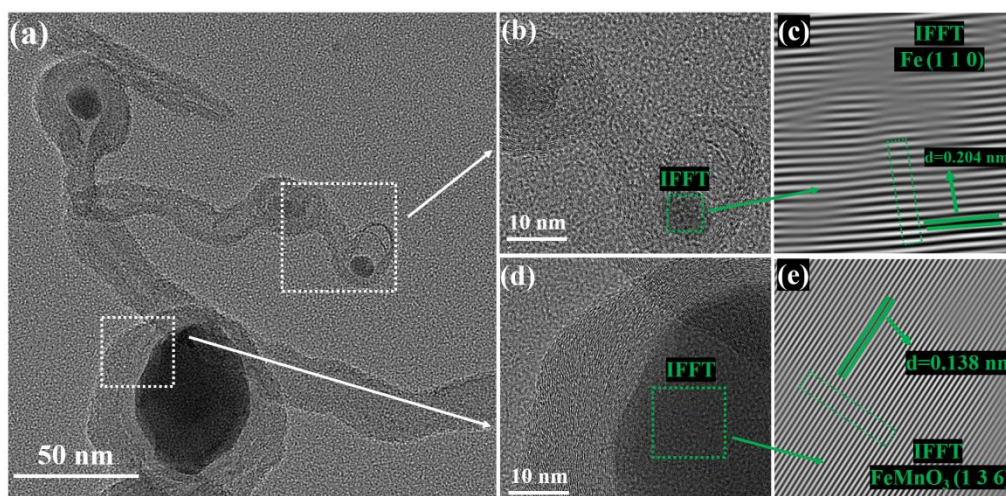


Figure S4: TEM image (a) and HRTEM images (b, d) for Z-Fe1Mn1-NC; IFFT images of the marked region of (b) and (d) are given in (c) and (e).

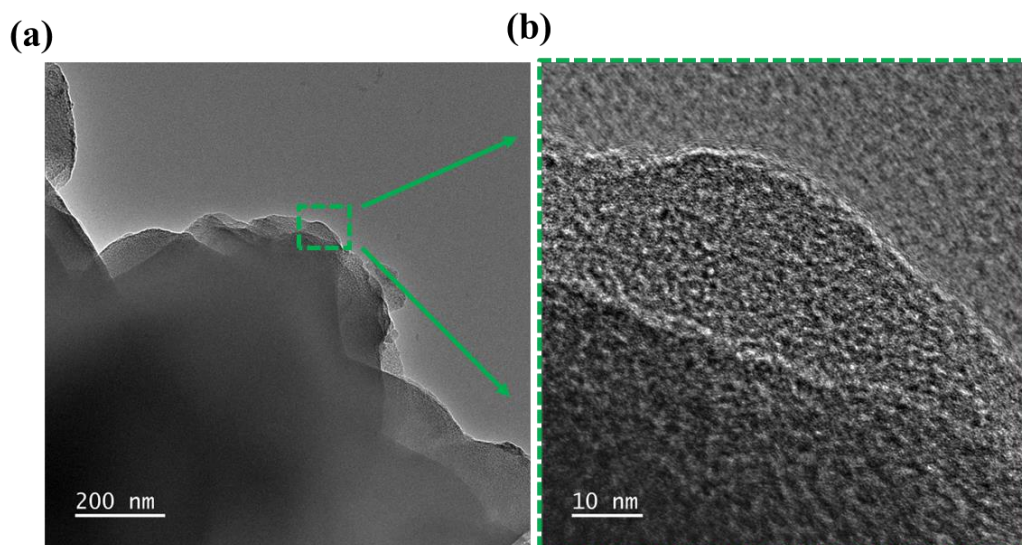


Figure S5: TEM image (a) and high-resolution TEM image (b) of NC.

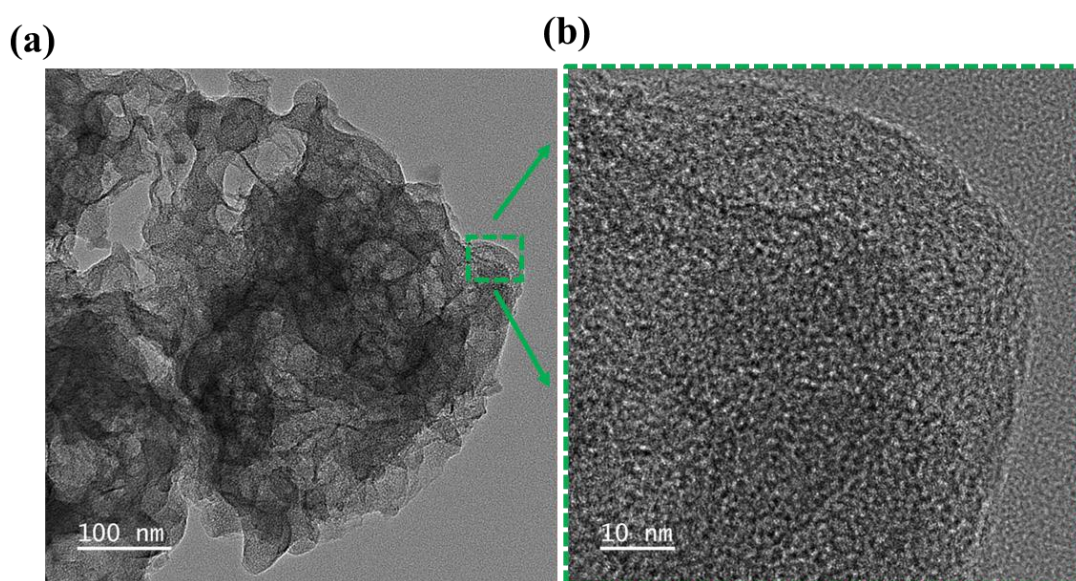


Figure S6: TEM image (a) and high-resolution TEM image (b) of Mn-C.

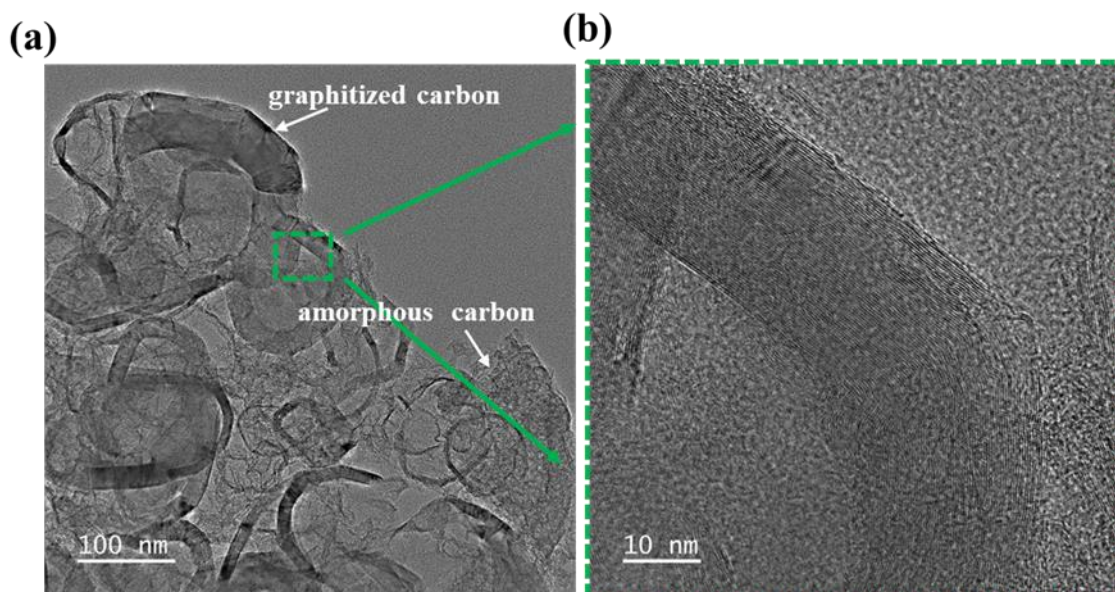


Figure S7: TEM image (a) and high-resolution TEM image (b) of Fe-C.

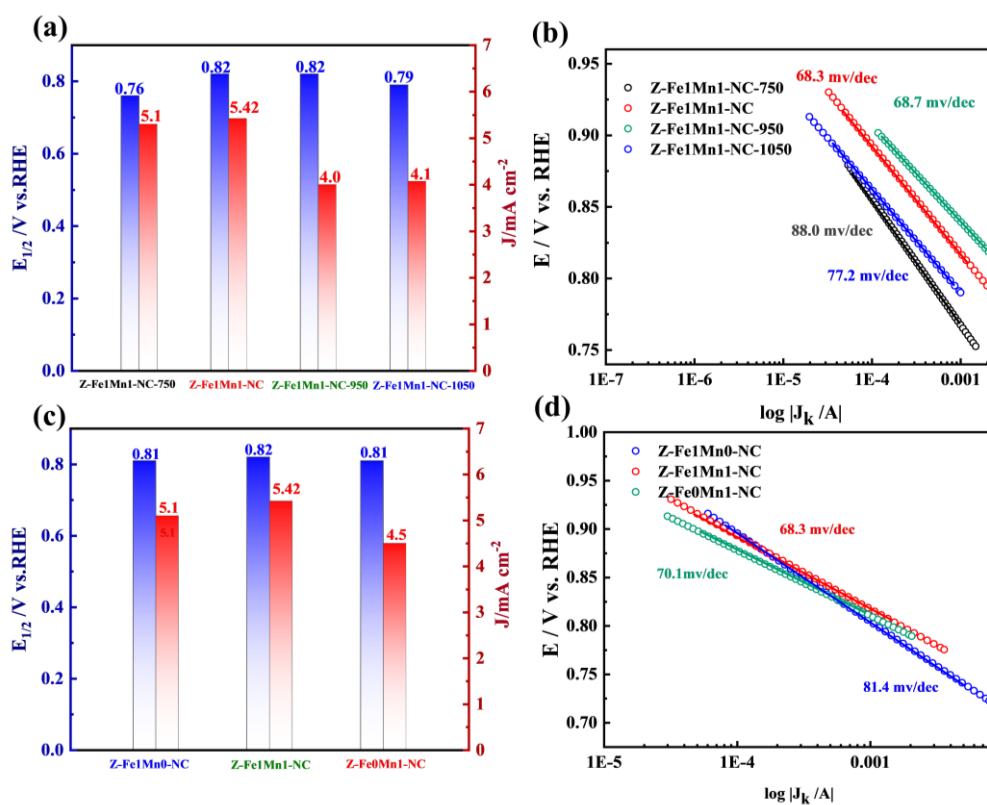


Figure S8: ORR performance in alkaline medium (0.1 M KOH). (a) Half-wave potentials $E_{1/2}$ and limiting current density J_L , and (b) corresponding Tafel curves of Z-Fe1Mn1-NC-750, Z-Fe1Mn1-NC, Z-Fe1Mn1-NC-950 and Z-Fe1Mn1-NC-1050. (c) Half-wave potentials $E_{1/2}$ and limiting current density J_L , and (d) corresponding Tafel curves of Z-Fe1Mn0-NC, Z-Fe1Mn1-NC and Z-Fe0Mn1-NC.

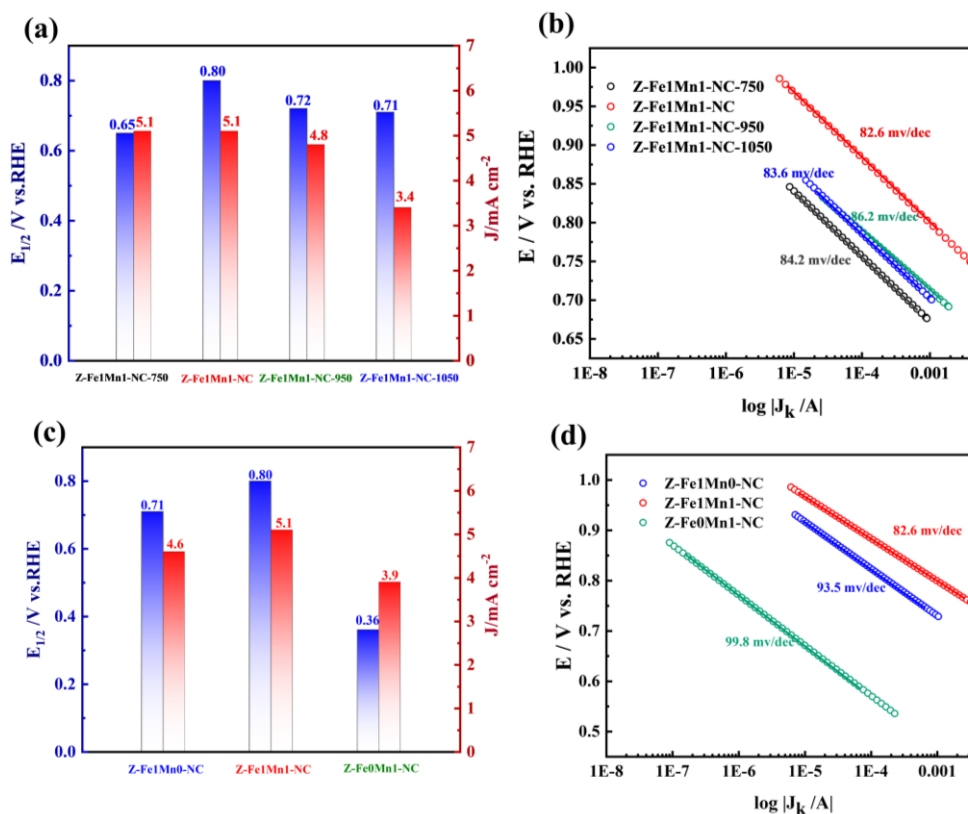


Figure S9: ORR performance in acidic medium (0.1 M HClO₄). (a) Half-wave potentials $E_{1/2}$ and limiting current density J_L , and (b) corresponding Tafel curves of Z-Fe1Mn1-NC-750, Z-Fe1Mn1-NC, Z-Fe1Mn1-NC-950 and Z-Fe1Mn1-NC-1050. (c) Half-wave potentials $E_{1/2}$ and limiting current density J_L , and (d) corresponding Tafel curves of Z-Fe1Mn0-NC, Z-Fe1Mn1-NC and Z-Fe0Mn1-NC.

Table S1. Summary of BET specific surface areas for various catalysts.

Samples	Total-BET area (m ² g ⁻¹)	Micro-BET area (m ² g ⁻¹)	Meso-BET area (m ² g ⁻¹)
NC	346.6	280.4	66.2
Fe-C	535.3	415.8	119.5
Mn-C	713.6	604.2	109.4
FeMn-C	673.4	442.6	230.8
Z-Fe1Mn1-NC	802.2	570.9	231.3

Table S2. Summary of element content for various catalysts.

Samples	C at. %	O at. %	N at. %	Fe at. %	Mn at. %	Zn at. %
NC	76.05	7.35	15.28	/	/	1.32
Fe-C	95.35	4.65	/	/	/	/
Mn-C	91.92	6.41	1.66	/	/	/
FeMn-C	93.92	3.95	2.13	/	/	/
Z-Fe1Mn1-NC	76.24	9.29	13.03	0.28	0.08	1.08

Table S3. Summary of fitting results for C 1s XPS spectra for various catalysts.

Samples	C-C/C=C (~284.8 eV) Proportion (at. %)	C-N/C-O (~286.1 eV) Proportion (at. %)	O-C=O (~288.4 eV) Proportion (at. %)	C 1s plasmon (~291.2 eV) Proportion (at. %)
NC	59.28	27.47	11.25	2.00
Fe-C	64.44	24.33	5.90	5.32
Mn-C	56.68	26.06	11.42	5.84
FeMn-C	67.96	22.22	6.95	2.87
Z-Fe1Mn1-NC	48.89	30.76	15.86	4.49

Table S4. Summary of fitting results for N 1s XPS spectra for various catalysts.

Samples	pyridinic-N (~398.7 eV) Proportion (at.%)	M-Nx (~399.8 eV) Proportion (at.%)	pyrrolic-N (~400.4 eV) Proportion (at.%)	graphitic-N (~401.3 eV) Proportion (at.%)	N-O1 (~402-403 eV) Proportion (at.%)	N-O2 (~405 eV) Proportion (at.%)
NC	38.01	16.73	12.73	14.18	12.54	5.81
Mn-C	55.02	/	18.42	/	18.15	8.41
FeMn-C	35.42	/	33.51	11.07	6.82	13.18
Z-Fe1Mn1-NC	42.51	24.63	11.54	9.89	5.94	5.49

Table S5. The fitting results for Fe 2p XPS spectra for Z-Fe1Mn1-NC.

Samples	Fe-Nx 2p 3/2 (~708.6 eV) Proportion (at.%)	Fe ²⁺ 2p 3/2 (~709.8 eV) Proportion (at.%)	Fe ³⁺ 2p 3/2 (~711.5 eV) Proportion (at.%)	Fe ²⁺ 2p 3/2 shakeup (~714.5 eV) Proportion (at.%)	Fe ³⁺ 2p 3/2 shakeup (~717.8 eV) Proportion (at.%)
Z-Fe1Mn1-NC	10.73	34.70	21.89	16.05	16.63

Table S6. The fitting results for Mn 2p XPS spectra for Z-Fe1Mn1-NC.

Samples	Mn ²⁺ 2p 3/2 (~640.9 eV) Proportion (at.%)	Mn ²⁺ satellite (~645.6 eV) Proportion (at.%)	Mn ²⁺ 2p 1/2 (~653.3 eV) Proportion (at.%)
Z-Fe1Mn1-NC	40.69	1.71	57.59

Table S7 Performance comparison of ORR activities for Fe-based nonprecious catalysts both in acidic and alkaline medium.

Catalysts	Electrolytes $E_{1/2}$ / V vs. RHE	Stability (J/J_0 / Time)	Electrolytes $E_{1/2}$ / V vs. RHE	Stability (J/J_0 /Time)	Ref.
Z-Fe1Mn1-NC	0.1M HClO ₄ 0.80	86.0% 15 h	0.1M KOH 0.82	91.0% 15 h	This work.
Mn-Fe@NCNTs	0.1M HClO ₄ 0.760	90.1% 8.05h	0.1M KOH 0.872	95.4% 8.05 h	Journal of Alloys and Compounds 953 (2023) 169992
FeMn(mIm)-N-C	0.1M HClO ₄ 0.778	/	0.1M KOH 0.861	92.0% 5.56 h	Journal of Colloid and Interface Science 642 (2023) 800–809
Fe&Mn/N-C	0.1M HClO ₄ 0.781	77.0% 2.8 h	0.1M KOH 0.904	77.0% 2.8 h	Small 2022, 18, 2200911
Fe-Mn-N-C	0.1M HClO ₄ 0.79	94.0% 13.8 h	0.1M KOH 0.93	96.0% 13.8 h	Applied Catalysis B: Environmental 317 (2022) 121770
Fe,Mn/N-C	0.1M HClO ₄ 0.804	92.6% 11.1 h	0.1M KOH 0.928	82.0% 11.1 h	NATURE COMMUNICATIONS (2021) 12:1734
FeNPC	0.1M HClO ₄ 0.735	90.3% 10 h	0.1M KOH 0.904	92.2% 10 h	Nano Research 2022, 16 (2), 1810- 1819.
FeNSC-ZM	0.5 M H ₂ SO ₄ 0.640	90.0% 11 h	0.1M KOH 0.840	90.0% 13.8 h	Chemical Engineering Journal 444 (2022) 136433
Fe,Mn,N-FGC	0.5 M H ₂ SO ₄ 0.74	/	0.1M KOH 0.89	67% 12 h	Inorg Chem 2020, 59 (7), 5194-5205
Fe ₃ Mn ₁ /N-CNTs- 100	0.1M HClO ₄ 0.57	/	0.1M NaOH 0.865	96.1% 2.8 h	ChemCatChem 2018, 10 (23), 5475- 5486.

Table S8 Performance comparison of Zn-air batteries for Fe-based nonprecious catalysts as air cathode.

Catalysts	Open-circuit potentials(V)	Power density (mW/cm ²)	Specific capacity(mAh/g)	Ref.
Z-Fe1Mn1-NC	1.475	164.3	708.3	This work.
FeMn(mIm)-N-C	1.518	160	735	Journal of Colloid and Interface Science 642 (2023) 800–809
Fe/Mn-N/C-RPB	1.35	141.12	/	Chemical Engineering Science 259 (2022) 117811
Fe5C2/Mn, N, S-CNTs	1.521	153.19	/	Journal of Colloid and Interface Science 647 (2023) 1–11
Mn-Fe@NCNTs	1.487	139.2	774.0	Journal of Alloys and Compounds 953 (2023) 169992
Fe,Mn/N-C	1.40	160.8	902	NATURE COMMUNICATIONS (2021) 12:1734
Fe-Se/NC	1.47	135	764	Angew. Chem. Int. Ed.2023,62,e202219191
Fe-N-C	1.47	111.7	821.8	Journal of Electroanalytical Chemistry 936(2023)117381
CoFe-NCNFs	1.522	116.1	/	Journal of Power Sources 521 (2022) 230926